The Correlation Between Galaxy HI Linewidths and K' Luminosities

Barry Rothberg[1], Will Saunders[2], R. Brent Tully[1], and Peter L. Witchalls[2,3]
[1] Institute for Astronomy, University of Hawaii, 2680 Woodlawn Drive, Honolulu, HI 96822 e-mail: tully@ifa.hawaii.edu
[2] Institute for Astronomy, University of Edinburgh, Royal Observatory, Blackford Hill, Edinburgh EH9 3HJ, Scotland, UK
[3] Deceased

ABSTRACT

The relationship between galaxy luminosities and rotation rates is studied with total luminosities in the K' band. Extinction problems are essentially eliminated at this band centered at 2.1μm. A template luminosity–linewidth relation is derived based on 65 galaxies drawn from two magnitude-limited cluster samples. The zero-point is determined using 4 galaxies with accurately known distances. The calibration is applied to give the distance to the Pisces Cluster (60 Mpc) at a redshift in the CMB frame of 4771 km s^{-1}. The resultant value of the Hubble Constant is 81 km s^{-1}Mpc^{-1}. The largest sources of uncertainty arises from the small number of zero-point calibrators at this time at K' and present application to only one cluster.

Subject headings: cosmology: distance scale – galaxies: fundamental parameters – distances

1. Luminosity – Linewidth Correlations

There is a strong correlation between the total luminosities of galaxies and the global rotation velocities (Tully & Fisher 1977). The correlation can be applied to give distances to galaxies. The rotation parameter gives an expectation luminosity and the apparent luminosity falls off from this value as the square of the distance. Aaronson, Huchra, & Mould (1979) noted the advantages of *infrared* luminosities: obscuration is minimized and the light comes from old stars which have less stochastic variability than the young stars. There is a substantial correlation between color and luminosity for spirals so the detailed correlations between luminosity and the rotation rate parameter depend on wavelength (Tully, Mould, & Aaronson 1982), steepening toward the infrared.

The original demonstration of the correlation used photographic or B band data while the Aaronson et al. collaboration pioneered work at aperture H band (1.6μm). In recent years, there has been a great deal of work at intermediate bands; either in the red where the contrast against the sky background is optimal (Pierce & Tully 1988, 1992; Willick 1991; Courteau 1996) or at I band where obscuration effects are the most diminished within the spectral domain accessible to CCD cameras (Pierce & Tully 1988, 1992; Han 1992; Mathewson, Ford, & Buchhorn 1992; Giovanelli et al 1997).

Since the seminal aperture photometry work by Aaronson et al., there has been only limited work at longer wavelengths (eg, Peletier & Willner 1991, 1993) although electronic imagers have become available with reasonably large formats. The primary disadvantage at wavelengths greater than 1 micron is the strong and variable atmospheric emission. All but the very centers of the highest surface brightness galaxies

emit below the flux levels of the sky. Our experience is at K', (2.1μm) a shift of the K band to avoid thermal emission (Wainscoat & Cowie 1992). One observes several scalelengths farther out in a galaxy at R or I than at K' with a fixed integration at the same telescope focus (Tully et al. 1996). On the other hand, there is the considerable advantage that obscuration problems are almost eliminated by K' (25% of the I extinction according to Tully et al. 1998). If extinction can be largely negated then one can restrict to samples that are highly inclined which minimizes the corrections required for projection effects in the kinematic parameter. Arguably the most dangerous potential systematic effects arise out of uncertain inclination and extinction corrections. Hence, although the correlations at K' are no better than at I and are a lot more work to acquire, they do eliminate some systematic problems. The first order of business is to see if one gets the same results across the spectrum from blue to infrared bands.

2. K' Photometry of the Separate Samples

Our strategy parallels the optical band procedures described by Tully & Pierce (1999; hereafter TP). Template luminosity – HI profile linewidth correlations are produced for magnitude-limited cluster samples. In the present case, data are available for two clusters. We vary the assumed differential distance modulus between clusters until an rms minimization is achieved with a linear regression slope to the common data set. The regression takes errors to be in linewidths, the prescription described by TP to avoid the Malmquist (1920) bias caused by a magnitude limit. The absolute scale of the correlation is set by least squares fit of the template relation to the luminosity–linewidth properties of a small number of galaxies with accurate independent distances.

2.1. The Ursa Major Cluster

The Ursa Major Cluster is as close to home as the Virgo or Fornax clusters but it is much more irregular, with no defined center, and a dynamical collapse time not much less than the age of the universe. The 79 known members are predominantly HI-rich disk systems, similar to those found in low density environments. The sample was discussed by Tully et al. (1996) and the data used in the current paper are presented in that earlier publication. There are 38 galaxies with $I < 13.4$ (after corrections), inclination $i \geq 45°$ and type Sa or later. The same sample is used to study optical band luminosity–linewidth correlations by TP and we use the same HI profile and inclination information. The small corrections for extinction as a function of galaxy inclination are those described by Tully et al. (1998). The tiny corrections for Galactic extinction are derived from the selected reddening given by Schlegel, Finkbeiner, & Davis (1998); we take $A^b_{K'} = 0.37E(B-V)$. The relevant data are gathered together in Table 1.

2.2. The Pisces Cluster

The sample to be considered is a spatially restricted subset of the material discussed by TP. The Perseus-Pisces filament is a prominent structure at roughly 5,000 km s^{-1} that includes several Abell and other clusters. The study of optical correlations by TP drew galaxies from a 20° length of the filament. Here we consider 27 galaxies drawn from the restricted range $0^h49^m < R.A. < 1^h32^m$. There are several sub-condensations of galaxies in this so-called Pisces Cluster but the structure is irregular and probably dynamically young overall. Sakai, Giovanelli, & Wegner (1994) identify separate NGC 383 and NGC 507

groups within this region. TP failed to find any differential in distances between separate components.

The K' photometry to be used is published here for the first time although it was involved in the analysis by Tully et al. (1998). The observations were made on 10 November, 1995, with the University of Hawaii 2.2m telescope on Mauna Kea. A 1024x1024 HgCdTe detector provided a field of 193 arcsec with 0.19 arcsec pixels. Five dithered 60 sec exposures were combined. The observing sequence would run sky - object 1 - object 2 - sky - object3 - object4 - sky ... Hence object observations were always either immediately preceded or followed by sky observations so there could be proper subtraction of the sky background. Pixel to pixel variations are eliminated using a combination of dome and sky flats. Dithered images were registered and median filtered to eliminate defects.

Reductions were carried out with IRAF routines. Once contaminating sources were masked, elliptical isophotes were fit progressively with radius, exponential disks were fit, and fluxes were extrapolated to infinity to give total magnitudes.

The small reddening corrections follow the same prescriptions mentioned in the previous sub-section. The HI profile information and inclinations are again the same as those used in the optical study of TP. The relevant material is presented in Table 1.

2.3. Zero-Point Calibrators

A special set-up provides a very wide field for K' observations. The University of Hawaii 0.61m telescope is used to piggyback an 0.25m telescope that feeds the 1024x1024 HgCdTe detector. The set-up gives a 29 arcmin field with 1.69 arcsec pixels. This field of view is greater than the dimensions of all galaxies in the northern sky with the exceptions of M31 and M33.

Observations of many of the largest galaxies were undertaken 6-11 February, 1997. Among the galaxies successfully observed, there are four that have accurate independent distances. Cepheid variables have been observed in NGC 3031 (Freedman et al. 1994: $(m-M)_0 = 27.80$), NGC 3198 (Kelson et al. 1999: $(m-M)_0 = 30.80$), NGC 3627 (Saha et al. 1999; Gibson et al. 1999: $(m-M)_0 = 30.06$), and NGC 4258 (Maoz et al. 1999: $(m-M)_0 = 29.54$). HI line profile information is available for each of these galaxies. The 4 galaxies are among the expanded set of calibrators used in the TP optical band study.

The observing strategy with the small telescope is similar to that used with the 2.2m telescope except the exposures extend over an hour per object so more frequent excursions are needed between object and sky. We observe in the pattern object - sky north - object - sky south - object - sky east - object - sky west (5 object, 4 sky). Exposures were 120 seconds and the pattern was repeated twice per object, resulting in a cumulative on-target exposure of 20 minutes.

Reduction procedures are similar between the observations taken with the large and small telescopes except for a caveat about flat fielding. Dome flats are not possible with the 0.25m telescope because the dome is not sufficiently out of focus. The observations with the small telescope were obtained remotely and we were not successful with twilight flats during the run in question. Hence flats were exclusively generated by median filtering all the off-object frames.

Adjustments for inclination and extinction within our galaxy follow the same recipes previously mentioned. Again, inclination and HI linewidth information is taken from TP. This material is gathered in Table 1.

3. Tabulated Data

The data is accumulated in Table 1 and provides information comparable to that in a table in TP. The following information is provided in each column. (1) Principal Galaxies Catalogue (PGC) number from the Lyon Extragalactic Database. (2) Alternative names; by preference, NGC (N), UGC (U), Zwicky (Z). (3) Morphological types (T:1,3,5,7,9=Sa,Sb,Sc,Sd,Sm). (4) Systemic velocity in the rest frame of the cosmic microwave background. (5) Galactic foreground extinction coefficient, $E(B-V)$. (6) Axial ratio of minor axis to major axis, q. (7) Inclination, i. (8) Total magnitudes, K'_T. (9) Total magnitudes adjusted for galactic extinction (b), inclination-dependent extinction (i), and k-correction (k), K'^{bik}_T. (10) Absolute magnitudes at the accepted distance modulus, $M^{bik}_{K'}$. (11) HI linewidth, W_{20}. (12) Linewidth uncertainty. (13) Logarithm of adjusted linewidth, $\log W^i_R$. (14) References for HI linewidths.

HI linewidth references are given by a 3 figure code. If the code is less than 600 then the reference is provided by Huchtmeier & Richter (1989) for that code. We have been maintaining a database that follows on from Huchtmeier & Richter and the additional references of concern are given here: 601 = Begeman (1989), 619 = Magri (1990), 630 = Haynes & Giovanelli (1991*a*), 631 = Haynes & Giovanelli (1991*b*), 637 = Roth et al. (1991), 655 = Schneider et al. (1992), 660 = Broeils (1992), 700 = Wegner et al. (1993), 701 = Haynes et al. (1997), 702 = Haynes, private communication, 706 = Giovanelli et al. (1997), 707 = Tully & Verheijen (1997).

4. The K' Luminosity–Linewidth Template Relation

In the two panels of Figure 1, one sees apparent magnitudes plotted against a logarithmic linewidth parameter for the two separate clusters. The linewidth parameter is derived from the 21 cm HI profile width and approximates $2V_{max}$, where V_{max} is the rotation curve maximum velocity (Tully & Fouqué 1985). Within type and inclination limits, the Ursa Major sample is complete to $I^{bik}_T = 13.4^m$ and the Pisces sample is almost complete to $I^{bik}_T = 13.8^m$ (where I_T magnitudes are extrapolated to infinity and the superscripts indicate corrections have been made for Galactic and internal extinction and the redshift effect).

In Figure 2, the Pisces sample has been shifted 2.55^m to achieve a best fit with the Ursa Major data. The fitting procedure is described in TP. Here is a brief review. Least squares fits are made with errors taken in linewidths, the procedure that nulls the Malmquist bias that arises with magnitude-limited samples. (Naive application of the regression with errors in magnitude to give distances would result in biased distances $\sim 10\%$ low.) A fit is made to the Ursa Major data alone, and the slope is force fit to the Pisces data to obtain a preliminary offset. Once this offset is applied, a fit is made to the combined data sets, then the new fit is applied separately to the two clusters to determine a residual difference. The Pisces offset is corrected by the residual, the process is repeated, and convergence is rapidly achieved. The best fit is illustrated by the dashed line in Fig. 2. The rms scatter of the 65 points is $\pm 0.44^m$.

5. The Zero–Point Calibration

Accurate distances are known for 4 galaxies with K' apparent magnitude and HI linewidth information: NGC 3031, NGC 3198, NGC 3627, and NGC 4258. The intrinsic luminosity–linewidth relation for the four systems is shown in Figure 3. The dashed line has the slope derived from the Ursa Major + Pisces template

and a zero-point that minimizes the sum of the deviations squared. This line is described by the formula:

$$M_{K'}^{bik} = -23.13(\pm 0.12) - 8.78(\pm 0.33)(\log W_R^i - 2.5) \tag{1}$$

The 1σ error on the slope is derived from the 2 cluster fit. The error on the zero-point is derived from the constraint from the 4 galaxies with Cepheid distances. The rms scatter of the four points is $\pm 0.22^m$.

The fit of the template data to the absolute calibration is seen in Figure 4. This fit requires a distance modulus for the Ursa Major Cluster of 31.31 and a modulus for Pisces of 33.86.

6. Distances to Additional Galaxies

Ten additional galaxies were observed at K' with the 0.25m aperture wide field arrangement. The absolute calibration of the K' luminosity–linewidth correlation given by Eq. (1) can be used to establish the distances of these galaxies. Information about these systems is provided in Table 2. The format of this table resembles that of Table 1 with small differences. The systemic velocities are the V_{GSR} values of the Third Reference Catalogue (de Vaucouleurs et al. 1991) rather than velocities in the frame of the microwave background and the absolute magnitudes are calculated from Eq. (1). There are two additional HI profile references: 613 = Cayatte et al. (1990) and 638 = Rupen (1991).

From the scatter in the luminosity–linewidth plots, the rms uncertainty for an individual modulus is judged to be $\pm 0.4^m$. The corrected linewidth for NGC 2841 is larger than the value for any of the calibrator or template systems. Hence application to this galaxy involves an extrapolation of the luminosity–linewidth correlation.

7. The Hubble Constant

The constraints on the Hubble Constant provided by TP are more restrictive but this first determination with the K' correlation is worth noting. The Ursa Major Cluster is strongly disturbed from Hubble expansion by its proximity to the Virgo Cluster but the Pisces Cluster is distant enough that its velocity may predominantly reflect the Hubble flow. The velocity of this cluster in the microwave background frame is 4771 km s^{-1} (Han & Mould 1992) and the distance from the K' calibration is 59 Mpc, whence $\mathrm{H}_0 = 81$ km s^{-1}Mpc^{-1}.

The statistical errors in this determination of H_0 are dominated by the small number of zero-point calibrators. A reduced χ^2 goodness of fit is presented in Figure 5. The 95% probability limits on the Hubble Constant *from this uncertainty alone* are ± 9.

There is limited value in exploring all the potential uncertainties in the current analysis because the same issues are addressed in TP, but in that paper we use many more template galaxies, more calibrators, and more clusters extending to larger velocities. The present K' sample is a subset of the optical sample and we use the same HI profile and inclination information. With so many factors held the same, we are able to see if there are any significant systematics due only to the photometry. In particular, the K' version has little sensitivity to extinction. The scale difference is a remarkably small 0.03^m, a 1% distance effect (the 1σ uncertainty with the use of only 4 calibrators is 5%). The analysis at B, R, I bands by TP gives $\mathrm{H}_0 = 77$ with essentially the entire difference a result of extending the analysis to include twelve clusters.

8. In Memorium

Our colleague Peter Witchalls carried out the photometric reductions of the Pisces sample. Sadly, he died before he saw the results of his effort.

Table 1. Data for 4 Calibrators and 2 Clusters

PGC	Name	Ty	V_{3K}	$E(B-V)$	b/a	Inc	K'_T	$K'^{\rm bik}_T$	$M^{\rm bik}_{K'}$	W_{20}	e$_{20}$	$\log W^i_R$	HI References
Zero-Point Calibrators: 4 galaxies with independent distances													
28630	N 3031	2	48	0.080	0.54	59.	3.55	3.44	−24.36	444	7	2.676	80 102 185 296
30197	N 3198	5	880	0.013	0.42	68.	7.79	7.71	−23.09	321	5	2.484	80 183 373 480 523 601
34695	N 3627	3	1066	0.032	0.61	54.	5.87	5.80	−24.26	381	5	2.626	80 113 183 373 473 515
39600	N 4258	4	657	0.016	0.36	72.	5.23	5.10	−24.44	442	5	2.628	183 373 387 442 473 480
Ursa Major: 38 galaxies, distance modulus = 31.31													
34971	U 6399	9	1002	0.015	0.28	78.	11.09	11.04	−20.27	173	20	2.153	373
35202	U 6446	7	826	0.016	0.62	53.	11.50	11.47	−19.84	156	9	2.193	157 373 706
35616	N 3718	1	1174	0.014	0.42	68.	7.47	7.36	−23.95	481	5	2.678	80 372 373 417 441 442
35676	N 3726	5	1079	0.017	0.62	53.	7.96	7.91	−23.40	294	6	2.504	80 203 373 387 429 480
35711	N 3729	2	1249	0.011	0.66	50.	8.60	8.56	−22.75	279	15	2.496	441
35999	N 3769	3	947	0.023	0.33	75.	9.10	9.01	−22.30	263	8	2.366	387 417 631
36343	U 6667	6	1170	0.017	0.15	90.	10.81	10.72	−20.59	199	11	2.212	373 387 706
36699	N 3877	5	1114	0.023	0.22	84.	7.75	7.60	−23.71	359	7	2.507	373 387 429 660 706
36825	U 6773	9	1124	0.017	0.50	62.	11.23	11.21	−20.10	119	7	2.026	630 655
36875	N 3893	5	1176	0.021	0.65	51.	7.84	7.79	−23.52	312	5	2.546	80 203 373 387 417 660
37036	N 3917	6	1158	0.022	0.23	83.	9.08	8.95	−22.36	295	6	2.412	201 373 387 660 702
37037	U 6816	9	1055	0.014	0.69	47.	11.91	11.89	−19.42	141	7	2.184	373 515
37038	U 6818	7	1033	0.022	0.28	78.	11.70	11.65	−19.66	176	12	2.161	373 387
37290	N 3949	4	1009	0.021	0.63	52.	8.43	8.38	−22.93	286	6	2.495	373 387 442 706
37306	N 3953	4	1241	0.030	0.50	62.	7.03	6.94	−24.37	426	5	2.641	183 373 387 416 660 706
37466	N 3972	4	1014	0.014	0.28	78.	9.39	9.29	−22.02	266	11	2.367	373 387
37525	U 6917	7	1113	0.027	0.58	57.	10.30	10.26	−21.05	202	8	2.295	373 387
37542	N 3985	9	1157	0.026	0.70	53.	10.19	10.16	−21.15	179	10	2.257	377 417 619
37553	U 6923	8	1248	0.028	0.40	69.	11.04	10.99	−20.32	174	6	2.176	373 387 436 515
37617	N 3992	4	1230	0.029	0.50	62.	7.23	7.13	−24.18	479	5	2.697	80 183 203 373 387 436
37691	N 4013	3	1064	0.017	0.22	84.	7.68	7.51	−23.80	409	7	2.570	373 473 701
37697	N 4010	7	1116	0.025	0.16	90.	9.22	9.08	−22.23	276	7	2.375	373 387 706
37719	U 6973	2	947	0.021	0.39	70.	8.23	8.13	−23.18	346	10	2.514	707
37735	U 6983	6	1263	0.027	0.64	52.	10.52	10.48	−20.83	197	7	2.310	157 373 387 706
38068	N 4051	4	928	0.013	0.75	50.	7.86	7.83	−23.48	267	8	2.475	80 116 373
38283	N 4085	5	945	0.018	0.26	80.	9.20	9.08	−22.23	304	7	2.430	373 387 407 442 619 706
38302	N 4088	4	952	0.020	0.38	71.	7.46	7.35	−23.96	373	5	2.548	373 387 407 442 619
38356	U 7089	8	1007	0.015	0.20	87.	11.11	11.06	−20.25	159	7	2.104	373 459
38370	N 4100	4	1272	0.023	0.30	77.	8.02	7.88	−23.43	404	9	2.573	373 387 442 706
38375	U 7094	8	1011	0.013	0.36	72.	11.58	11.57	−19.74	112	20	1.967	655
38392	N 4102	2	1021	0.020	0.57	57.	7.86	7.80	−23.51	328	11	2.537	373 387 637
38643	N 4138	1	1105	0.014	0.63	52.	8.19	8.14	−23.17	329	10	2.566	140 241 619
38795	N 4157	3	963	0.021	0.19	90.	7.52	7.33	−23.98	425	7	2.586	373 387 706
38988	N 4183	6	1158	0.015	0.16	90.	9.76	9.63	−21.68	256	7	2.338	201 373 706
39237	N 4218	9	923	0.016	0.60	55.	10.83	10.80	−20.51	156	8	2.182	158 293 347 619
39241	N 4217	3	1234	0.017	0.27	79.	7.61	7.46	−23.85	421	13	2.589	158 373 387 512 706
39285	N 4220	1	1136	0.018	0.31	76.	8.36	8.23	−23.08	372	15	2.535	619
40537	N 4389	4	925	0.015	0.68	49.	9.12	9.09	−22.22	192	8	2.317	346 373 387 619
Pisces filament: 27 galaxies, distance modulus = 33.86													
2865	U 501	5	4769	0.061	0.14	90.	10.31	10.08	−23.78	404	8	2.557	452 543
2899	U 509	5	4825	0.061	0.42	68.	12.41	12.33	−21.53	236	10	2.324	452
2928	U 511	5	4287	0.060	0.22	85.	12.25	12.10	−21.76	310	9	2.430	384 452
2964	Z501-024	5	4686	0.066	0.22	85.	12.56	12.43	−21.43	257	15	2.336	565
3020	U 525	3	4621	0.060	0.59	56.	11.52	11.46	−22.40	242	7	2.386	452 543
3108	U 540	3	4661	0.053	0.57	57.	11.13	11.06	−22.80	289	7	2.470	452 543
3133	U 542	5	4205	0.056	0.20	90.	10.00	9.81	−24.05	397	7	2.549	452 543
3222	U 557	3	4192	0.060	0.42	68.	11.90	11.80	−22.06	295	8	2.437	452 543
3235	U 556	3	4318	0.057	0.20	90.	10.28	10.09	−23.77	414	8	2.569	452 543
3260	N 295	3	5163	0.062	0.40	69.	9.05	8.91	−24.95	475	15	2.663	543
3274	N 296	5	5340	0.064	0.28	78.	11.72	11.61	−22.25	257	9	2.343	452 543
3336	U 575	4	4346	0.061	0.16	90.	11.51	11.33	−22.53	323	17	2.449	452 543

Table 1—Continued

PGC	Name	Ty	V_{3K}	$E(B-V)$	b/a	Inc	K'_T	$K'^{\rm bik}_T$	$M^{\rm bik}_{K'}$	W_{20}	e_{20}	$\log W^i_R$	HI References
3606	U 623	1	4529	0.059	0.41	69.	10.66	10.54	−23.32	395	15	2.576	452 543
3611	N 338	2	4479	0.055	0.35	73.	9.04	8.88	−24.98	564	8	2.734	452 543
3664	U 633	3	5272	0.064	0.25	82.	10.76	10.58	−23.28	422	7	2.581	452 543
3866	U 669	5	5556	0.070	0.22	85.	10.95	10.81	−23.05	281	15	2.380	452 543
4110	U 714	5	4345	0.064	0.72	45.	10.86	10.81	−23.05	258	15	2.487	452
4561	N 444	5	4544	0.064	0.26	80.	11.52	11.39	−22.47	293	8	2.407	452 543
4563	U 809	5	3920	0.059	0.18	90.	11.37	11.19	−22.67	346	14	2.483	543 700
4596	N 452	2	4670	0.066	0.29	78.	9.40	9.22	−24.64	528	12	2.693	452 543
4735	U 841	4	5287	0.062	0.22	84.	11.48	11.33	−22.53	312	8	2.433	452 543
5035	N 494	2	5168	0.061	0.35	73.	9.35	9.19	−24.67	527	15	2.701	452
5061	N 496	4	5722	0.072	0.55	59.	10.53	10.44	−23.42	340	20	2.539	452
5284	U 987	1	4373	0.060	0.32	75.	9.72	9.57	−24.29	416	8	2.586	452 543
5344	N 536	3	4911	0.052	0.33	74.	8.80	8.63	−25.23	549	10	2.719	543 700
5440	U 1033	5	3757	0.051	0.18	90.	10.75	10.56	−23.30	367	7	2.512	452 543
5702	N 582	3	4070	0.053	0.24	82.	9.62	9.43	−24.43	474	7	2.638	452 543

Table 2. Distance Derivations for 10 Galaxies

PGC	Name	Modulus	Ty	$E(B-V)$	b/a	Inc	K'_T	$K'^{\rm bik}_T$	$M^{\rm bik}_{K'}$	W_{20}	e_{20}	$\log W^i_R$	HI References
24930	N 2683	30.09	3	0.033	0.25	81.	6.16	5.99	−24.09	440	5	2.609	183 373 377 473 660
26512	N 2841	31.85	3	0.015	0.45	66.	6.19	6.07	−25.77	614	4	2.801	183 373 442 473 522
33550	N 3521	30.31	4	0.058	0.50	62.	5.64	5.53	−24.77	468	5	2.687	183 373 393 473 515
39028	N 4192	31.08	2	0.035	0.21	86.	6.94	6.74	−24.33	470	5	2.636	151 373 375 509 613
39422	N 4244	28.67	6	0.021	0.20	90.	7.69	7.59	−21.07	221	7	2.265	373 442
42002	N 4559	29.03	6	0.018	0.40	69.	7.12	7.05	−21.97	256	5	2.368	201 373 442 660
42038	N 4565	30.42	3	0.015	0.22	85.	5.79	5.59	−24.82	528	5	2.692	183 373 473 638
42637	N 4631	28.79	7	0.017	0.22	85.	6.18	6.04	−22.74	322	6	2.455	183 222 373
45948	N 5033	31.07	5	0.012	0.47	64.	6.62	6.52	−24.54	450	4	2.660	183 390 515 523 562
46153	N 5055	29.54	4	0.017	0.52	61.	5.44	5.36	−24.17	400	5	2.618	183 373 374 473 480

REFERENCES

Aaronson, M., Huchra, J.P., & Mould, J.R. 1979, ApJ, 229, 1

Begeman, K.G 1989, A&A, 223, 47

Broeils, A.H. 1992, Ph.D. thesis, University of Groningen

Cayatte, V., van Gorkom, J.H., Balkowski, C., & Kotanyi, C. 1990, AJ, 100, 604

Courteau, S. 1996, ApJS, 103, 363

de Vaucouleurs, G., de Vaucouleurs, A., Corwin, H.G. Jr., Buta, R.J., Paturel, G., & Fouqué, P. 1991, Third Reference Catalogue of Bright Galaxies, (New York: Springer-Verlag)

Freedman, W.L. Hughes, S.M., Madore, B.F., Mould, J.R., Lee, M.G., Stetson, P.B., Kennicutt, R.C., Turner, A., Ferrarese, L., Ford, H., Graham, J.A., Hill, R., Hoessel, J.G., Huchra, J., and Illingworth, G.D. 1994, Ap.J., 427, 628.

Gibson, B.K, Stetson, P.B., Freedman, W.L., Mould, J.R., Kennicutt, R.C. Jr., Huchra, J.P., Sakai, S., Graham, J.A., Fassett, C.I., Kelson, D.D., Ferrarese, L., Hughes, S.M., Illingworth, G.D., Macri, L.M., Madore, B.F., Sebo, K.M., & Silbermann, N.A. 1999, ApJ, astro-ph/9908192

Giovanelli, R., Haynes, M.P., Herter, T., Vogt, N.P., Wegner, G., Salzer, J.J., da Costa, L.N., & Freudling, W. 1997, AJ, 113, 22

Han, M.S. 1992, ApJS, 81, 35

Han, M.S. & Mould, J.R. 1992, ApJ, 396, 453

Haynes, M.P., & Giovanelli, R. 1991*a*, ApJS, 77, 337

Haynes, M.P., & Giovanelli, R. 1991*b*, AJ, 102, 841

Haynes, M.P., Giovanelli, R., Herter, T., Vogt, N.P., Freudling, W., Maia, M.A.G., Salzer, J.J., & Wegner, G. 1997, AJ, 113, 1197

Huchtmeier, W. & Richter, O-G. 1989, *A General Catalogue of HI Observations of Galaxies* (Springer-Verlag)

Kelson, D.D., Illingworth, G.D., Saha, A., Graham, J.A., Stetson, P.B., Freedman, W.F., Kennicutt, R.C.Jr., Mould, J.R., Ferrarese, L., Huchra, J.P., Madore, B.F., Prosser, C.F., Bresolin, F., Ford, H.C., Gibson, B.K., Hoessel, J.G., Hughes, S.M.G., Macri, L.M., Sakai, S. and Silbermann, N.A. 1999, ApJ, 514, 614

Magri, C. 1990, Ph.D. thesis, Cornell University

Maoz, E., Newman, J.A., Ferrarese. L., Stetson, P.B., Zepf, S.E., Davis, M., Freedman, W.L., & Madore, B.F. 1999, Nature, 401, 451

Mathewson, D.S, Ford, V.L, & Buchhorn, M. 1992, ApJS, 81, 413

Peletier, R.F, & Willner, S.P. 1991, ApJ, 382, 315

Peletier, R.F, & Willner, S.P. 1993, ApJ, 418, 626

Pierce, M.J., & Tully, R.B. 1988, ApJ, 330, 579

Pierce, M.J., & Tully, R.B. 1992, ApJ, 387, 47

Roth, J., Mould, J.R., & Davies, R.D. 1991, AJ, 102, 1303

Rupen, M.P 1991, AJ, 102, 48

Saha, A., Sandage, A., Tammann, G.A., Labhardt, L., Macchetto, F.D., & Panagia, N. 1999, ApJ, 522, 802

Sakai, S., Giovanelli, R., & Wegner, G. 1994, ApJ, 108, 33

Schlegel, D.J., Finkbeiner, D.P., & Davis, M. 1998, ApJ, 500, 525

Schneider, S.E., Thuan, T.X., Mangum, J.G., & Miller, J. 1992, ApJS, 81, 5

Tully, R.B., & Fisher, J.R. 1977, A&A, 54, 661

Tully, R.B., & Fouqué, P. 1985, ApJS, 58, 67

Tully, R.B., Mould, J.R, & Aaronson, M. 1982, ApJ, 257, 527

Tully, R.B., and Pierce, M.J. 1999, ApJ, submitted (TP)

Tully, R.B., Pierce, M.J., Huang, J.S., Saunders, W., Verheijen, M.A.W., & Witchalls, P.L. 1998, AJ, 115, 2264

Tully, R.B., & Verheijen, M.A.W. 1997, ApJ, 484, 145

Tully, R.B., Verheijen, M.A.W., Pierce, M.J., Huang, J.S., & Wainscoat, R.J. 1996, AJ, 112, 2471

Wainscoat, R.J, & Cowie, L.L. 1992, AJ, 103, 332

Wegner, G., Haynes, M.P., & Giovanelli, R. 1993, AJ, 105, 1251

Willick, J.A. 1991, Ph.D. thesis, Univ. of California, Berkeley.

This preprint was prepared with the AAS LATEX macros v4.0.

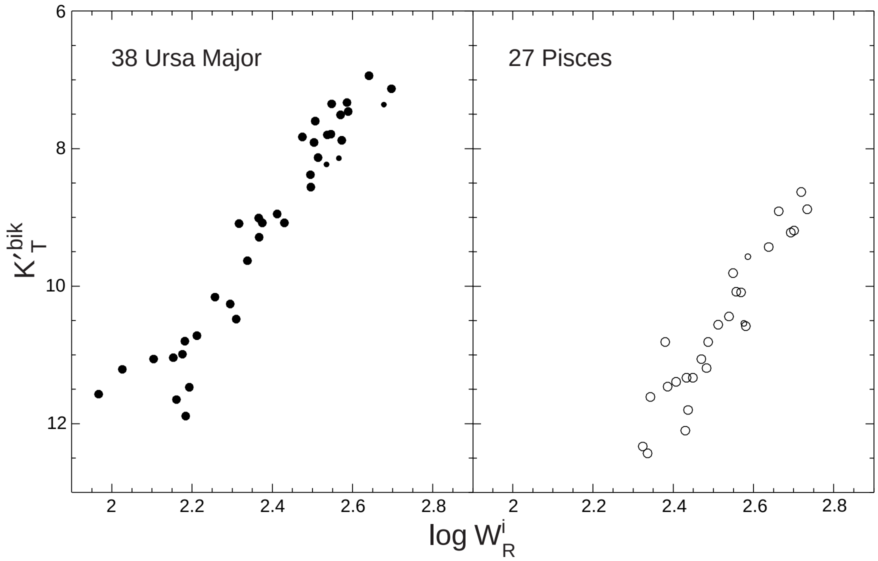

Fig. 1.— K'-band apparent magnitude–HI profile linewidth plots for the two clusters that contribute to the template luminosity–linewidth correlations. Magnitudes are adjusted for internal and Galactic absorption and small redshift corrections. Large symbols: types Sab and later. Small symbols: type Sa. The Ursa Major sample is complete to $I_T^{bik} = 13.4$. The Pisces sample is nearly complete to $I_T^{bik} = 13.8$. Galaxies fainter than these limits are excluded.

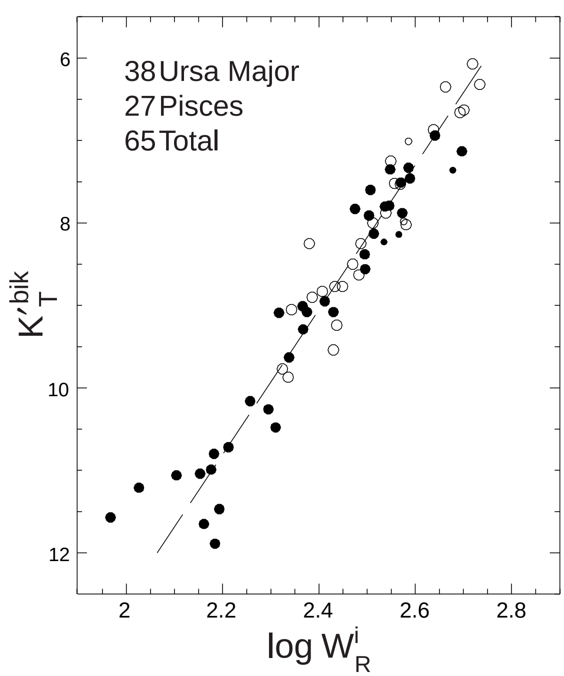

Fig. 2.— K'-band apparent magnitude–linewidth relation for 2 clusters with the Pisces sample translated 2.55^m to match the Ursa Major relation. Symbols as in Fig. 1. The straight line is a least squares fit to the ensemble with errors in linewidths after the iterations described in the text.

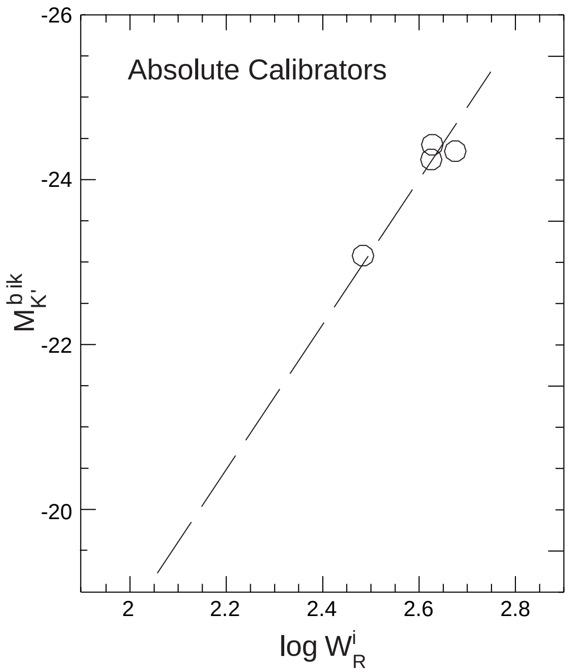

Fig. 3.— K' absolute magnitude–linewidth relation for 4 galaxies with independently determined distances from application of the cepheid period–luminosity relation. The straight line is the least squares best fit slope shown in Fig. 2 shifted to fit the calibrators.

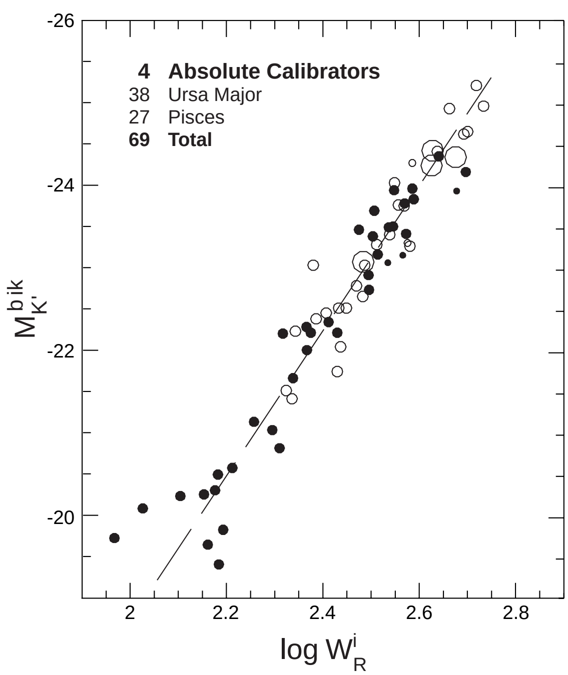

Fig. 4.— K' absolute magnitude–linewidth relation with the cluster template galaxies translated to overlay on the zero-point calibrator galaxies ($(m-M)_{UMa} = 31.31$; $(m-M)_{Pisc} = 33.86$). Symbols and straight line fits as in previous plots.

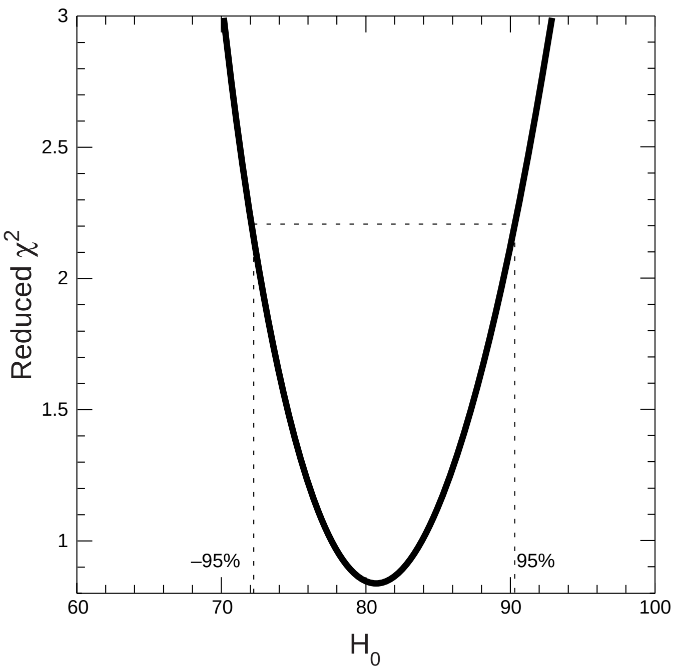

Fig. 5.— Reduced χ^2 goodness of fit dependency on the choice of H_0 associated with the constraints provided by the 4 calibrators.